



## Quantification of margins and mixed uncertainties using evidence theory and stochastic expansions

Harsheel Shah <sup>a,\*</sup>, Serhat Hosder <sup>a</sup>, Tyler Winter <sup>b</sup>

<sup>a</sup> Aerospace Simulations Laboratory, Department of Mechanical and Aerospace Engineering, Missouri University of Science & Technology, 1870 Miner Circle, 258A Toomey Hall, Rolla, MO 65409, USA

<sup>b</sup> M4 Engineering Inc., 4020 Long Beach Blvd, Long Beach, CA 90807, USA



### ARTICLE INFO

#### Article history:

Received 21 February 2014

Received in revised form

15 October 2014

Accepted 15 January 2015

Available online 31 January 2015

#### Keywords:

Evidence theory

Polynomial chaos

Point collocation

Margins and uncertainty quantification

Representation of uncertainty

Reliability

System safety

### ABSTRACT

The objective of this paper is to implement Dempster–Shafer Theory of Evidence (DSTE) in the presence of mixed (aleatory and multiple sources of epistemic) uncertainty to the reliability and performance assessment of complex engineering systems through the use of quantification of margins and uncertainties (QMU) methodology. This study focuses on quantifying the simulation uncertainties, both in the design condition and the performance boundaries along with the determination of margins. To address the possibility of multiple sources and intervals for epistemic uncertainty characterization, DSTE is used for uncertainty quantification. An approach to incorporate aleatory uncertainty in Dempster–Shafer structures is presented by discretizing the aleatory variable distributions into sets of intervals. In view of excessive computational costs for large scale applications and repetitive simulations needed for DSTE analysis, a stochastic response surface based on point-collocation non-intrusive polynomial chaos (NIPC) has been implemented as the surrogate for the model response. The technique is demonstrated on a model problem with non-linear analytical functions representing the outputs and performance boundaries of two coupled systems. Finally, the QMU approach is demonstrated on a multi-disciplinary analysis of a high speed civil transport (HSCT).

© 2015 Elsevier Ltd. All rights reserved.

### 1. Introduction

The objective of this paper is to implement Dempster–Shafer Theory of Evidence (DSTE) in the presence of mixed (aleatory and multiple sources of epistemic) uncertainty to the reliability and performance assessment of complex engineering systems through the use of quantification of margins and uncertainties (QMU) methodology. Specifically, *uncertainty quantification* (UQ) has been used as a tool of *certification* to decide whether a system is likely to perform safely and reliably within design specifications. The unique contributions of the current study to the system reliability and safety research can be summarized as follows: the current work focuses on the creation of a novel QMU framework in terms of Dempster–Shafer structures (belief and plausibility) for the characterization of uncertainty in system design performance as well as the performance boundaries to obtain uncertainty and margin metrics to evaluate the system safety and reliability. Specifically, DSTE is used for uncertainty quantification to address the possibility of multiple sources and intervals for epistemic uncertainty characterization. Furthermore, the

DSTE is utilized for mixed uncertainty quantification by discretizing the aleatory probability distributions into optimum sets of intervals and treating them as well-characterized epistemic variables. In addition, the response quantities of interest for design performance and boundaries are represented with stochastic surrogates based on non-intrusive polynomial chaos to reduce the computational expense of implementing DSTE for uncertainty quantification of high-fidelity complex system models.

To review the previous work and contrast with the current study, the following section gives a detailed literature review on QMU methodology, epistemic and aleatory uncertainty considerations in QMU, and DSTE for epistemic and mixed uncertainty representation. In [Section 3](#), we briefly discuss different types of uncertainties present in a computational model. [Section 4](#) gives an overview of basics of point-collocation non-intrusive polynomial chaos (NIPC) methodology. In [Section 5](#), we present the mathematical framework for Dempster–Shafer Theory of Evidence for mixed uncertainty quantification using NIPC response surface. [Section 6](#) describes the incorporation of uncertainty measures of evidence theory into QMU. The newly developed QMU approach is demonstrated in [Section 7](#) on a model problem with non-linear analytical functions representing the outputs and performance boundaries of two coupled systems. In [Section 8](#), the proposed QMU methodology is demonstrated on a multi-disciplinary

\* Corresponding author. Tel.: +1 908 803 3257.

E-mail address: [hrsvff@mst.edu](mailto:hrsvff@mst.edu) (H. Shah).

Nomenclature	
$M$	margin
$U$	uncertainty
$FU$	upper boundary performance
$U_{FU}$	uncertainty in $FU$
$FL$	lower boundary performance
$U_{FL}$	uncertainty in $FL$
$F$	performance at design condition
$U_F$	uncertainty in $F$
$M_{UP}$	upper margin
$M_{LW}$	lower margin
$\tilde{M}$	Mach number
$\tilde{\alpha}$	angle of attack
$\lambda$	taper ratio
$\Lambda$	sweep angle
$n$	number of random variables
$N_S$	number of samples
$n_p$	over-sampling ratio
$\overline{p}$	order of polynomial chaos
$\xi$	standard input random variable vector
$N_t$	number of terms in a total-order expansion
$\psi$	random basis function
$\alpha$	coefficient in polynomial chaos expansion
$\alpha^*$	stochastic function
$Bel$	belief
$Pl$	plausibility
$\mathbb{U}$	Universal set
$\mathcal{U}$	set of focal elements of $\mathbb{U}$
BPA	basic probability assignment
$m(\epsilon)$	BPA corresponding to subset $\epsilon$ of $\mathcal{U}$
$P$	belief/plausibility/probability level
$\gamma$	confidence level

analysis of a supersonic civil transport. Section 9 concludes the paper by summarizing the findings of the current study.

## 2. Literature review

### 2.1. QMU methodology and confidence ratio

QMU is a methodology developed to facilitate analysis and communication of confidence for certification of complex systems, which is performed with quantified uncertainty and margin metrics obtained for various system responses and performance parameters. In the recent years, a number of studies were reported on the theoretical development and the application of the QMU concept in the certification of reliability and safety of nuclear weapons stockpile [1–5]. The description of the key elements of a QMU framework that can be used to address risk and risk mitigation for the certification of nuclear weapons was presented by Sharp and Wood-Schultz [1]. Eardley [3] described QMU as a formalism dealing with the reliability of complex technical systems and the confidence that can be placed in estimates of reliability. They also investigated the main components (performance gates, margins, and uncertainties) of the QMU methodology. Key ideas underlying the concept of QMU were defined by Pilch et al. [6]. They claimed that QMU provides input for a risk-informed decision making process and constitutes a decision-support methodology for complex technical decisions that are made under conditions of uncertainty.

Pepin et al. [7] presented a practical QMU metric for the certification of complex systems in terms of the ratio of margin ( $M$ ) and uncertainty ( $U$ ), known as confidence ratio (CR) or confidence factor. The metric allowed uncertainty both on the operating region and the performance requirement and was not restrictive to a probabilistic definition of the uncertainty. A study by Lucas et al. [8] utilized the QMU methodology to study the reliability of a ring structure. According to the author, if  $U$  denotes a suitable measure of uncertainties and has been quantified accurately, the confidence ratio may be taken as a rational basis for certification. Also, a QMU approach based on confidence ratio was used for the characterization of the operation limits of the supersonic combustion engine of a hypersonic air-breathing vehicle by Iaccarino et al. [9]. Some previous work have expressed a concern for the use of confidence ratio as the sole indicator of confidence [10]. Pilch et al. [6] expressed dissatisfaction with the confidence ratio metric being deceptively simple and involving significant loss of information.

Compared to the previous work, the current study is expected to contribute to the QMU methodology by efficient implementation of DSTE for the calculation of margins and uncertainties, which is the primary focus of the paper. Following some previous studies, the current work also utilizes confidence ratio as a measure of system safety in the demonstration of the UQ and QMU methodologies developed, however more sophisticated measures utilizing the UQ methodology introduced in this paper could be investigated and integrated to the QMU framework in future studies.

### 2.2. Epistemic and aleatory uncertainty considerations in QMU

As implied in the previous section where the QMU methodology is reviewed, one should not forget that *uncertainty quantification* (determination of output uncertainty resulting from uncertainty in inputs) is a broad research area on which the QMU process is dependent. Uncertainties in engineering systems can be characterized mainly as aleatory (inherent or irreducible) uncertainty and epistemic (reducible) uncertainty originating due to lack of knowledge. Pilch et al. [6] emphasized the need to separate aleatory and epistemic uncertainty in QMU. Helton [11] presented a comprehensive study on QMU, which included a detailed analysis of the QMU concept with different representations of uncertainty. Oberkampf et al. [12] have described various methods for estimating total uncertainty by identifying all possible sources of variability, uncertainty and error in computational simulations. Urbina et al. [13] proposed a methodology to quantify the margins and uncertainty in presence of mixed uncertainties through a framework based on Bayes networks and further developed a QMU metric in terms of probability of failure. A new formalism based on Bayesian inference, known as probabilistic QMU or pQMU, was introduced by Wallstrom [14], which was fully probabilistic and showed how QMU may be interpreted within the framework of system reliability theory. Epistemic uncertainty was represented using a Bayesian approach by transforming the bounds to probability density functions. Many have expressed concern about modeling epistemic uncertainty via probability density functions due to the assumption of a higher resolution of knowledge than what is really present [15]. Owhadi et al. [16] introduced a rigorous framework for UQ (optimal uncertainty quantification) that did not implicitly impose inappropriate assumptions on the characterization of uncertainty, which has been the weakness of most of the UQ methods. They further compared the framework with different UQ methods like Monte Carlo strategies, stochastic expansion methods, sensitivity analysis and Bayesian inference. However, the paper did not specifically discuss methods for different representation of epistemic

uncertainty such as possibility theory, interval analysis or evidence theory.

### 2.3. DSTE for epistemic and mixed uncertainty representation

As an alternative to Bayesian approach, formulation of mathematical structures like the evidence theory [17–19] has been an attractive approach for appropriate representation of epistemic uncertainty due to the fact that it does not make assumptions regarding the distribution of the variables described by intervals. DSTE approach is particularly useful when the uncertain variables are defined by more than one interval (i.e., multiple sources or expert opinions on uncertainty ranges). Probability theory and evidence theory were introduced as possible mathematical structures for the representation of the epistemic uncertainty associated with the performance of safety systems by Helton et al. [20]. The results suggested that evidence theory provided a valuable representational tool for the display of the implications of significant epistemic uncertainty in the inputs of complex systems. Furthermore, Helton et al. [21] explained the use of evidence theory as an alternative to the use of probability theory for the representation of epistemic uncertainty in QMU-type analyses. Swiler et al. [22] studied various approaches like interval analysis and DSTE in order to characterize epistemic uncertainty in the calculation of margins.

In previous years, extensive research has been dedicated to improve the practical application of the Dempster–Shafer theory to complex models due to the excessive computational cost associated with the required number of simulations [23–25]. A sampling based computational strategy for the representation of epistemic uncertainty in model predictions with evidence theory was introduced by Helton et al. [15] to reduce the computational cost of crude Monte Carlo method. In the present paper, a stochastic response surface constructed using point-collocation NIPC [26–30] has been implemented as a response surrogate in uncertainty analysis in order to reduce the computational cost.

Recently, Eldred et al. [31] have demonstrated mixed UQ using different methods like interval optimization, second-order probability [19,28,30,32] and DSTE. They investigated the use of nested sampling for mixed UQ, where each sample taken from the epistemic distributions at the outer loop results in an inner loop sampling over the aleatory probability distributions. In order to demonstrate the accuracy and efficiency over crude nested sampling, the mixed UQ results obtained through local gradient based and global non-gradient based optimization on the outer epistemic loop within nested sampling approach were compared. Recently, SENTZ and FERSON [33] proposed the use of probability bound analysis coupled with Dempster–Shafer theory for treating mixed uncertainty, as one of the tools relevant for QMU. In their work, the p-boxes [34] for aleatory uncertain parameters were discretized into 100 equiprobability levels in order to be represented as Dempster–Shafer structures. In the current paper, we propose to use the DSTE procedure for mixed UQ by discretizing the aleatory probability distributions into optimum sets of intervals (explained mathematically in Section 5) and treat them as well-characterized epistemic variables. For accurate representation in terms of Dempster–Shafer structures, these parameters are discretized into an optimum number of sets of intervals based on a previous study by Shah et al. [35]. This approach enables us to represent mixed uncertainty in terms of Dempster–Shafer structures for uncertainty analysis with multiple sources of uncertainty.

## 3. Types of uncertainty

Uncertainties are assigned to the specification of input physical parameters that are required for computational models. Two types of uncertainties exist in analyses of complex systems: aleatory

uncertainty and epistemic uncertainty. Many contributions have been dedicated to emphasize the importance of characterization and treatment of uncertainties in performance assessments (PAs) for complex systems [36–41]. Helton [42] illustrates the use of the Kaplan/Garrick ordered triple representation for risk in maintaining a distinction between aleatory (stochastic) and epistemic (subjective) uncertainty.

### 3.1. Aleatory uncertainty

Aleatory uncertainty, also known as probabilistic uncertainty, arises due to inherent physical variability present in the system being analyzed. It is not strictly due to lack of knowledge and is irreducible. Conducting additional experiments might provide more description of the variability but cannot be eliminated completely. For example, the Mach number can be treated as an aleatory uncertain variable in the computational aerodynamics analysis of airfoils or wings.

### 3.2. Epistemic uncertainty

The epistemic uncertainty arises due to lack of knowledge and is reducible by using, e.g., a combination of calibration, inference from experimental observations and improvement of the physical models. One source of epistemic uncertainty is the set of assumptions introduced in the derivation of mathematical models of the physical phenomena. This type of uncertainty cannot be defined in a probabilistic framework unless we assume a specific distribution which may lead to inaccurate results as shown by Oberkampf et al. [43]. Thus, epistemic variables are often modeled using intervals derived from experimental data or expert judgment with specified lower and the upper bounds. Turbulence modeling parameters (e.g., closure coefficients) in computational fluid dynamics (CFD) simulations present a good example for epistemic uncertainty.

## 4. Point-collocation non-intrusive polynomial chaos

Polynomial chaos is an uncertainty propagation approach which has been used in many recent UQ studies. In this work, we focus on generalized polynomial chaos using the Wiener–Askey scheme, which is explained in detail by Xiu and Karniadakis [44]. In previous years, many researchers have utilized polynomial chaos theory in stochastic computations [26–28,35,45,46]. In non-intrusive polynomial chaos expansion (PCE), simulations are used as black boxes and the calculation of chaos expansion coefficients is based on a set of simulation response evaluations. The point-collocation NIPC is derived from the polynomial chaos theory, which is based on spectral representation of uncertainty [47]. An important aspect of the spectral representation of uncertainty is that a stochastic response function can be decomposed into deterministic and stochastic components. Thus, for any stochastic response function  $\alpha^*$ , we can write,

$$\alpha^*(\vec{x}, \vec{\xi}) \approx \sum_{j=0}^P \alpha_j(\vec{x}) \psi_j(\vec{\xi}) \quad (1)$$

where  $\alpha_j(\vec{x})$  is the deterministic component and  $\psi_j$  is the random basis function corresponding to  $j$ th mode. Generally,  $\alpha^*$  is a function of deterministic variable vector  $\vec{x}$  and the  $n$ -dimensional independent standard random variable vector  $\vec{\xi} = (\xi_1, \dots, \xi_n)$ . In theory, the expansion given in Eq. (1) is an infinite series. However, in practice this series is truncated at a finite number of terms (hence the approximation sign used in Eq. (1) based on a selected expansion order and finite number of uncertain variables. The PCE can be created on a complete order. In this case, the total number of output modes

$(N_t)$  for an expansion order of  $p$  and  $n$  random variables is given by

$$N_t = P + 1 = \frac{(n+p)!}{n!p!} \quad (2)$$

An alternative approach as indicated by Eldred et al. [48] is to employ a ‘tensor-product expansion’, in which polynomial order bounds are applied on a per-dimension basis including all combinations of the one-dimensional polynomials. In this work, we employ total-order expansion from creating the polynomial chaos response surfaces. The basis functions used in Eq. (1) are optimal polynomials that are orthogonal with respect to a weight function over the support region of the input random variable vector. In terms of  $L^2$  convergence of the statistics, the Hermite polynomial is optimal for normal distribution whereas the Laguerre and Legendre polynomials are used for exponential and uniform input uncertainty distributions respectively. The detailed description of the orthogonal polynomials for different input uncertainty distributions (e.g., uniform, normal, exponential, etc.) and the associated weight functions are given by Hosder [29], Xiu and Karniadakis [44], and Eldred et al. [48].

The collocation based NIPC starts with replacing uncertain variables of interest with their polynomial expansions derived from Eq. (1). Next,  $P + 1 (N_t)$  vectors ( $\vec{\xi}_j = \{\xi_1, \xi_2, \dots, \xi_n\}_j, j = 0, 1, 2, \dots, P$ ) are sampled from the uncertainty space defined by the bounds of the uncertain variables with Latin Hypercube (LH) sampling for a given polynomial chaos expansion with number of modes determined from Eq. (2). The deterministic model (e.g., computational fluid dynamics model, finite element model, etc.) is evaluated at these points. With the left hand side of Eq. (1) known from the solutions of the deterministic model evaluations at the sample points, a linear system of equations can be obtained as

$$\begin{pmatrix} \psi_0(\vec{\xi}_0) & \psi_1(\vec{\xi}_0) & \dots & \psi_p(\vec{\xi}_0) \\ \psi_0(\vec{\xi}_1) & \psi_1(\vec{\xi}_1) & \dots & \psi_p(\vec{\xi}_1) \\ \vdots & \vdots & \ddots & \vdots \\ \psi_0(\vec{\xi}_P) & \psi_1(\vec{\xi}_P) & \dots & \psi_p(\vec{\xi}_P) \end{pmatrix} \begin{pmatrix} \alpha_0 \\ \alpha_1 \\ \vdots \\ \alpha_p \end{pmatrix} = \begin{pmatrix} \alpha^*(\vec{x}, \vec{\xi}_0) \\ \alpha^*(\vec{x}, \vec{\xi}_1) \\ \vdots \\ \alpha^*(\vec{x}, \vec{\xi}_P) \end{pmatrix} \quad (3)$$

Eq. (3) represents a linear system of equations which needs to be solved in order to determine the spectral modes  $\alpha_j$  ( $j = 0, 1, \dots, P$ ) for the stochastic function  $\alpha^*$ . Eq. (2) is considered as the minimum number of deterministic samples required to solve the linear system of equations. However, if more number of deterministic samples ( $N_S$ ) are available, the over-determined system is solved using a least squares approach. The term, over-sampling ratio denoted by  $n_p$  is related to Eq. (2) in the following manner:

$$N_S = n_p \times \frac{(n+p)!}{n!p!} \quad (4)$$

Thus, an  $n_p$  of 1 corresponds to the minimum number of deterministic samples required. Hosder et al. [26] demonstrated through different stochastic model problems that an  $n_p$  of 2 is the optimum value for most problems, which has also been implemented in the current study.

## 5. An approach for mixed UQ using evidence theory

This section summarizes the evidence theory traditionally used for pure epistemic analysis and extends this idea to perform mixed UQ analysis by converting the aleatory uncertain variables into Dempster–Shafer structures.

### 5.1. Fundamentals of evidence theory

Evidence theory introduces two new measures of uncertainty, belief (Bel), i.e., lower limit of probability and plausibility (Pl), i.e., upper limit of probability. Evidence theory application involves the

specification of  $(\mathbb{U}, \mathcal{V}, m)$  where  $\mathbb{U}$  denotes the universal set,  $\mathcal{V}$  denotes the collection of subsets or set of focal elements of  $\mathbb{U}$  and  $m$  is the basic probability assignment (BPA), which can be viewed as the belief of the user of how likely it is that the uncertain input falls within the specified interval. BPA, a value between 0 and 1, can be assigned for any possible subset of the universal set based on experimentation or expert opinion. The advantage of this theory is that it does not assume any particular value within the interval and nor does it assign a specific distribution to the interval. Also, Fig. 1 illustrates that the axiom of additivity is not imposed, as the evidential measure for the occurrence and negation of an event does not have to sum to unity ( $Bel(A) + Bel(\bar{A}) \leq 1$ ,  $Pl(A) + Pl(\bar{A}) \geq 1$ ,  $Bel(A) + Pl(\bar{A}) = 1$ ) where  $\bar{A}$  represents the negation of event  $A$ .

According to the definition,  $m(\varepsilon)$  denotes the BPA corresponding to subset  $\varepsilon$  of  $\mathcal{V}$ . Any additional evidence supporting the claim that the uncertain variable lies within a subset of  $\varepsilon$ , say  $B \subset \varepsilon$ , must be assigned another non-zero BPA  $m(B)$ .  $m(\varepsilon)$  should satisfy following axioms of evidence theory:

- $m(\varepsilon) > 0$  for any  $\varepsilon \in \mathcal{V}$ .
- $m(\varepsilon) = 0$  if  $\varepsilon \subset \mathbb{U}$  and  $\varepsilon \ni \mathcal{V}$ .
- $m(\emptyset) = 0$  where  $\emptyset$  denotes an empty set.
- $\sum m(\varepsilon) = 1$  for all  $\varepsilon \in \mathcal{V}$ .

In case of multiple sources of uncertainty per variable, the Dempster rule of combination has been extensively used with a strong assumption that there is some degree of consistency or agreement among the opinions of different sources. It has been proved by Yager [49] that the Dempster's rule completely ignores the conflict among different sources. Zadeh [50] in his review of Shafer's book, *A Mathematical Theory of Evidence*, pointed out that using Dempster's rule with conflicting evidences results in erroneous analysis. Thus, in our study, we adopt the mixing or averaging rule which generalizes the averaging operation used for probability distributions. The mathematical formulation is given by

$$m_{1\dots n}(A) = \frac{1}{n} \sum_{j=1}^n w_j m_j(A) \quad (5)$$

where  $m_j$ 's are the BPAs for belief structures being aggregated and  $w_j$ 's are the weights assigned according to the reliability of the sources. There is abundant literature dedicated to combination rules for the evidence theory [51,52] which is beyond the scope of this paper.

Once the uncertainty associated with the domain is characterized by an evidence space in the form of BPAs, an input sample space is constructed. For example, if  $y = f(\vec{x})$  where  $\vec{x} = [x_1, x_2, \dots, x_n]$  with the evidence space defined as  $(\mathbb{X}_i, \mathcal{X}_i, m_i)$  for each input uncertainty, the input sample space is given by

$$\mathbb{X} = \{x : x = [x_1, x_2, \dots, x_n] \in \mathbb{X}_1 \times \mathbb{X}_2 \times \dots \times \mathbb{X}_n\} \quad (6)$$

Further for  $\vec{x}$ , the evidence space can be defined by  $(\mathbb{X}, \mathcal{X}, m_X)$  where  $\mathcal{X}$  is developed from the sets contained in the following equation:

$$C = \{\varepsilon : \varepsilon = [\varepsilon_1, \varepsilon_2, \dots, \varepsilon_n] \in \mathcal{X}_1 \times \mathcal{X}_2 \times \dots \times \mathcal{X}_n\} \quad (7)$$

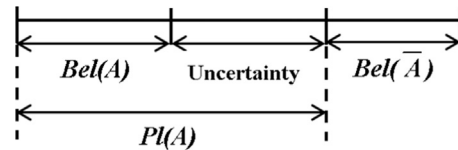


Fig. 1. Schematic of belief and plausibility.

Under the assumption that the  $x_i$  are independent,  $m_X$  is defined as

$$m_X(\varepsilon) = \begin{cases} \prod_{i=1}^n m_i(e_i) & \text{if } \varepsilon = \varepsilon_1 \times \varepsilon_2 \times \dots \times \varepsilon_n \in \mathcal{X} \\ 0 & \text{otherwise} \end{cases} \quad (8)$$

for subsets  $\varepsilon$  of  $\mathbb{X}$ .

Once the BPAs for input sample space in Eq. (6) are defined by Eq. (8), belief and plausibility for the output  $y$  can be evaluated as

$$\text{Bel}_Y(\varepsilon) = \sum_{S|S \in f^{-1}(\varepsilon)} m_X(S) \quad (9)$$

$$\text{Pl}_Y(\varepsilon) = \sum_{S|S \cap f^{-1}(\varepsilon) \neq \emptyset} m_X(S) \quad (10)$$

As no assumptions were made to calculate these measures, Bel and Pl provide a more realistic uncertainty structure consistent with the given evidences. The evidence theory statistics can be summarized in terms of cumulative belief and plausibility functions (CBF and CPF) and complementary cumulative belief and plausibility functions (CCBF and CCPF) as shown in Fig. 2.

These measures are calculated on the basis of minimum and maximum response values for each combination in the input sample space. Interval optimization approach (mathematical formulation given in Eq. (11)) can be implemented to provide accurate results for both, the original function or the response surface based on point-collocation NIPC, which is used as a surrogate of the original function in this work:

$$\begin{aligned} & \underset{x}{\text{minimize/maximize}} \quad f(\vec{\xi}) \\ & \text{subject to} \quad \vec{\xi}_L \leq \vec{\xi} \leq \vec{\xi}_U \end{aligned} \quad (11)$$

where  $f(\vec{\xi})$  is the required response value,  $\vec{\xi}_L$  and  $\vec{\xi}_U$  correspond to lower and upper bounds of the standard random variables. The final step is to calculate the belief and plausibility structures using the minimum and maximum response values according to Eqs. (9) and (10).

Now, if the uncertainty in output  $y$  is characterized by  $(\mathbb{Y}, \mathcal{Y}, m_Y)$ , the output uncertainty is summarized using CBF, CPF, CCBF and CCPF given by the following equations:

$$\text{CBF} = [\rho, \text{Bel}_X(f^{-1}(\mathbb{Y}_\rho))], \quad \rho \in \mathbb{Y} \quad (12)$$

$$\text{CCBF} = [\rho, \text{Bel}_X(f^{-1}(\mathbb{Y}_\rho))], \quad \rho \in \mathbb{Y} \quad (13)$$

$$\text{CPF} = [\rho, \text{Pl}_X(f^{-1}(\mathbb{Y}_\rho))], \quad \rho \in \mathbb{Y} \quad (14)$$

$$\text{CCPF} = [\rho, \text{Pl}_X(f^{-1}(\mathbb{Y}_\rho))], \quad \rho \in \mathbb{Y} \quad (15)$$

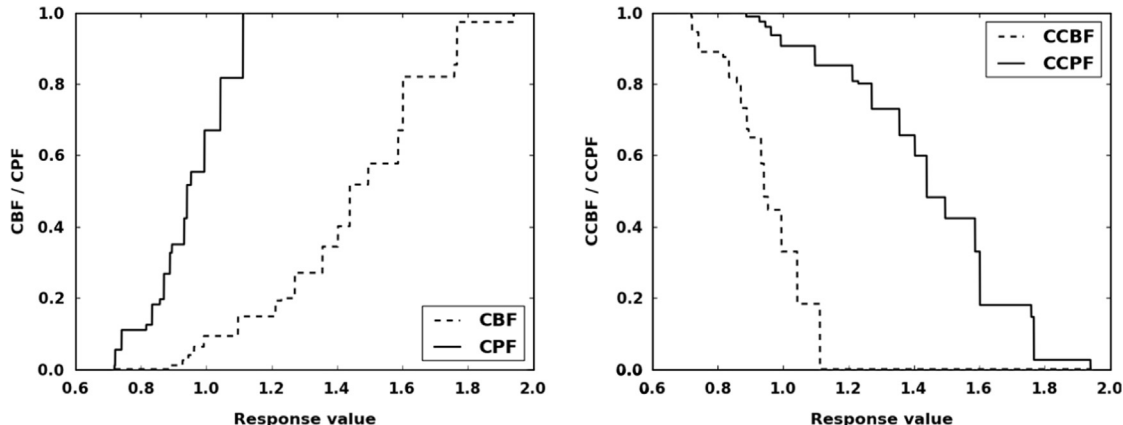


Fig. 2. Example of cumulative and complementary cumulative belief and plausibility functions.

where  $\mathbb{Y}_\rho = \{y : y \in \mathbb{Y} \text{ and } y > \rho\}$  and  $\mathbb{Y}_\rho^c = \{y : y \in \mathbb{Y} \text{ and } y \leq \rho\}$ . Detailed explanation of the evidence theory with numerical examples has been provided by Oberkampf et al. [43], Helton et al. [53] and Nikolaidis et al. [54].

### 5.2. Aleatory uncertainty representation in terms of Dempster–Shafer structures

Although Dempster–Shafer theory is primarily used for epistemic uncertainty representation, there may be instances when aleatory uncertainties are present in the model along with the epistemic. In that case, one may choose to segregate the aleatory uncertainties and treat them within an inner loop of nested sampling in which case we may end up with multiple belief and plausibility structures as shown by Eldred et al. [31] or one may choose to discretize the aleatory variables into sets of intervals according to their respective probability distributions.

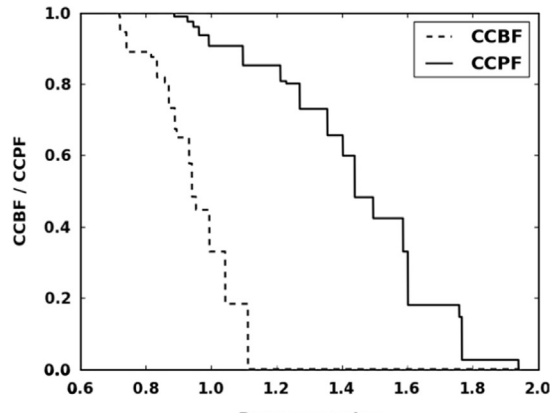
In this paper, we focus on the latter option of discretizing the aleatory variables into sets of intervals and assign BPAs to each interval corresponding to the probability distribution. Shah et al. [35] gave a detailed description of the methodology of aleatory uncertainty representation in terms of Dempster–Shafer structures. For example, a random variable with uniform distribution can be divided into  $n$  number of intervals with an equal BPA of  $1/n$  assigned to each sub-interval as can be seen in the right hand side plot of Fig. 3. Suppose  $x_1$  is a uniformly distributed variable with lower and upper bounds as  $[0.1, 0.7]$  and we discretize the same into 5 sub-intervals ( $n=5$ ). The Dempster–Shafer structure for  $x_1$  can be given by

$$x_1 = ([0.1, 0.22], m_1), ([0.22, 0.34], m_2), ([0.34, 0.46], m_3), \\ \dots ([0.46, 0.58], m_4), ([0.58, 0.7], m_5)$$

$$\text{where } m_i = \frac{1}{n} = \frac{1}{5} \quad (i = 1, 2, \dots, 5)$$

In order to discretize a random variable with normal distribution, we need to characterize the same with a lower bound and an upper bound. Consider the left plot in Fig. 3 which shows a standard normal distribution, i.e., with 0 mean ( $\mu = 0$ ) and 1 standard deviation ( $\sigma = 1$ ). As per the theory, for a normally distributed random variable with mean  $\mu$  and  $\sigma$  as the standard deviation, 99.7% of the area under the curve is within  $\mu \pm 3\sigma$ . Hence, this can be treated as a benchmark for bounding all the normal variables in our analysis. However, the BPA should be assigned to each sub-interval according to the Gaussian distribution by solving the definite integral in the following equation:

$$P(a < X < b) = \int_a^b f(X) dx \quad \text{where } f(X) = \frac{1}{\sigma\sqrt{2\pi}} \exp \frac{-(X-\mu)^2}{2\sigma^2} \quad (16)$$



where  $a$  and  $b$  denote the upper and lower bounds of the sub-interval and  $P(a < X < b)$  denotes the probability of  $X$  between  $a$  and  $b$ .

Suppose  $x_2$  is a normally distributed variable with a mean value of 0.5 ( $\mu = 0.5$ ) and standard deviation of 0.01 ( $\sigma = 0.01$ ). The lower and upper bounds for  $x_2$  using  $\mu \pm 3\sigma$  are [0.47, 0.53] and we decide to discretize the same into 3 intervals. The Dempster–Shafer structure for  $x_2$  can be given by

$$x_2 = ([0.47, 0.49], m_1), ([0.49, 0.51], m_2), ([0.51, 0.53], m_3)$$

where  $m_1 = 0.1573$ ,  $m_2 = 0.6827$  and  $m_3 = 0.1573$

In the current study, the interval discretization is based upon the convergence study performed by the authors [35] for the minimum number of intervals required to accurately capture the aleatory uncertainty in a model problem. The discretization process mainly depends upon the amount of information needed by the Dempster–Shafer structures to accurately cover the uncertainty domain.

## 6. QMU based on evidence theory

### 6.1. Key measures required for QMU

The key measures of the QMU framework to be developed are shown in Fig. 4. In this QMU framework, for the whole engineering system (e.g., aircraft or spacecraft) or for each sub-system, the first step will be to determine performance metrics (system outputs) relevant to the systems modeling, which should ideally be functions of all input parameters including the operating conditions. Then these metrics will be evaluated at a design condition determined for the safe and reliable operation of the engineering system. Each of these metrics  $F$  will typically involve some amount of uncertainty  $U_F$  due to the inherent real-life variation of parameters used in physical models as well as the epistemic uncertainties. The safe and reliable operation region of the spacecraft or aircraft (performance gates) will be bounded with a lower bound  $FL$  and an upper bound  $FU$  for each metric (i.e., metrics evaluated at the off-design boundaries), which will

also include some uncertainty ( $U_{FL}$  for  $FL$  and  $U_{FU}$  for  $FU$ ) due to the aforementioned uncertainty sources.

A measure of the distance between the design value of each performance metric and the lower boundary including the effect of uncertainties  $U_F$  and  $U_{FL}$  will give the lower margin  $M_{LW}$  and the distance between the upper boundary and the design value of each performance metric including the effect of uncertainties  $U_{FU}$  and  $U_F$  will give the upper margin  $M_{UP}$ . The margins must significantly exceed any associated uncertainty in order to avoid failure. Using the uncertainty ( $U$ ) and the margin ( $M$ ) information, a QMU metric has to be developed to quantify and certify the confidence for the safe operation of the system or each sub system (e.g., confidence ratio, CR) which is given by

$$CR = \frac{M}{U} \quad (17)$$

where  $M$  is a measure of the margin and  $U$  represents a measure of the uncertainty. The confidence ratio can be used as a degree to which the operation of a system or each sub-system is considered to lie within 'safe' bounds. As mentioned earlier, margins should exceed any associated uncertainty thereby stating that a CR sufficiently larger than 1 indicates safe and reliable conditions.

Since there exist two performance gates for each performance metric (upper and lower bounds), the evaluation of margin and uncertainty will result in two confidence ratios: (1) confidence ratio with respect to lower boundary  $CR_{LW}$  and (2) confidence ratio with respect to the upper boundary  $CR_{UP}$ . However, it is important to note that the CR is calculated for each system, sub-system and/or component of a sub-system in a particular QMU analysis. The system confidence ratio  $CR_{System}$  is represented by the minimum CR which replicates the worst case scenario as far as system safety is concerned. Theoretically speaking, there is a family of confidence ratios in a problem with mixed uncertainties due to the presence of multiple cumulative distribution functions (CDFs) per p-box. The bounding CDFs (lowest and highest) of the p-box are used to calculate the 95% confidence interval in uncertainty quantification [29]. Similar methodology is used to calculate the confidence ratio for the lower

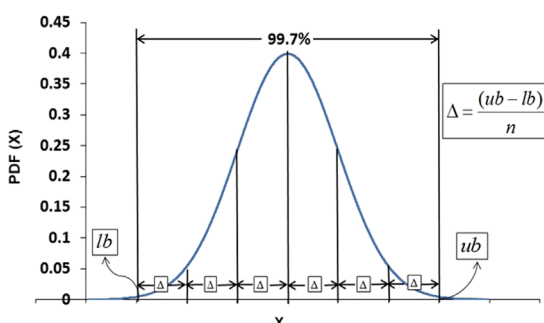


Fig. 3. Discretization of a normally and uniformly distributed variable.

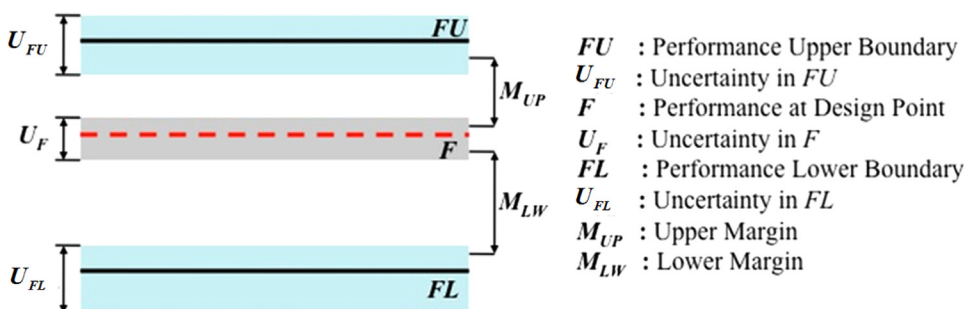
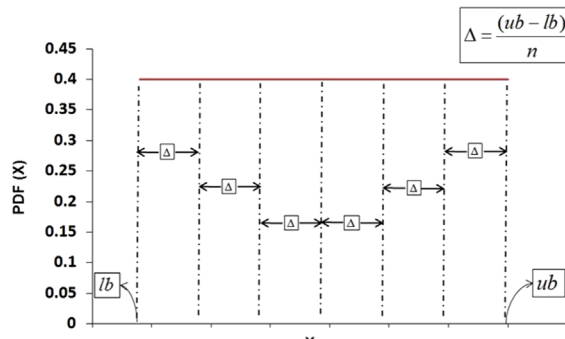


Fig. 4. Schematic of key measures used in a QMU framework.

and upper boundaries respectively. Further, the minimum value of the two CRs ( $CR_{LW}$  and  $CR_{UP}$ ) will result in the worst case scenario and a reliable value to carry out the performance assessment and certification.

Mathematically, the two confidence ratios can be formulated as follows:

$$CR_{LW} = \frac{M_{LW}}{U_{LW}} \quad \text{and} \quad CR_{UP} = \frac{M_{UP}}{U_{UP}} \quad (18)$$

In Eq. (18), similar to the measure of the margins,  $U_{UP}$  is a function of performance metric and upper boundary uncertainties, i.e.,  $U_F$  and  $U_{FU}$  whereas  $U_{LW}$  is a function of performance metric and lower boundary uncertainties, i.e.,  $U_F$  and  $U_{FL}$ . The system confidence ratio can be chosen to be the smallest out of the two performance gates. Thus, the minimum confidence ratio from among  $CR_{LW}$  and  $CR_{UP}$  is likely to tend towards the failure region and can be considered as the confidence ratio for the system.

## 6.2. QMU framework based on evidence theory

This section formulates the QMU framework in terms of evidence theory uncertainty measures, belief and plausibility. The usage of DSTE for QMU is preferred especially in situations where multiple sources of uncertainties are encountered for epistemic variables. If this is not the case and we have single source of uncertainty for both probabilistic and epistemic variables, then one can consider to perform mixed uncertainty quantification using methods like second order probability. When a problem formulation consists of probabilistic distributions along with Dempster–Shafer structures for epistemic variables, the discretization procedure as mentioned in Section 5.2 should be used for representing aleatory variables in terms of well-characterized epistemic variables.

Based on this discussion, four cases are presented for the formulation of uncertainty ( $U$ ) and margin ( $M$ ) calculations; (1) no uncertainty, (2) pure epistemic uncertainty, (3) pure aleatory uncertainty and (4) mixed (aleatory–epistemic) uncertainty. As this paper focuses

**Table 1**  
Formulations for uncertainty calculation with respect to upper boundary.

Type of uncertainty	$U_{UP1}(FU)$	$U_{UP2}(FU)$	$U_{UP3}(F)$	$U_{UP4}(F)$
No uncertainty	FU	FU	F	F
Pure epistemic	$Bel_P = 0.5$	$Pl_P = (1 - \gamma)/2$	$Bel_P = (1 + \gamma)/2$	$Pl_P = 0.5$
Pure aleatory	$FU_P = 0.5$	$FU_P = (1 - \gamma)/2$	$F_P = (1 + \gamma)/2$	$F_P = 0.5$
Mixed aleatory–epistemic	$Bel_P = 0.5$	$Pl_P = (1 - \gamma)/2$	$Bel_P = (1 + \gamma)/2$	$Pl_P = 0.5$

**Table 2**  
Formulations for uncertainty calculation with respect to lower boundary.

Type of uncertainty	$U_{LW1}(FL)$	$U_{LW2}(FL)$	$U_{LW3}(F)$	$U_{LW4}(F)$
No uncertainty	FL	FL	F	F
Pure epistemic	$Pl_P = 0.5$	$Bel_P = (1 + \gamma)/2$	$Pl_P = (1 - \gamma)/2$	$Bel_P = 0.5$
Pure aleatory	$FL_P = 0.5$	$FL_P = (1 + \gamma)/2$	$F_P = (1 - \gamma)/2$	$F_P = 0.5$
Mixed aleatory–epistemic	$Pl_P = 0.5$	$Bel_P = (1 + \gamma)/2$	$Pl_P = (1 - \gamma)/2$	$Bel_P = 0.5$

**Table 3**  
Formulations for margin calculation.

Type of uncertainty	$M_{UP1}(FU)$	$M_{UP2}(F)$	$M_{LW1}(F)$	$M_{LW2}(FL)$
No uncertainty	FU	F	F	FL
Pure epistemic	$Pl_P = (1 - \gamma)/2$	$Pl_P = (1 - \gamma)/2$	$Pl_P = (1 - \gamma)/2$	$Bel_P = (1 + \gamma)/2$
Pure aleatory	$FU_P = (1 - \gamma)/2$	$F_P = (1 - \gamma)/2$	$F_P = (1 - \gamma)/2$	$FL_P = (1 + \gamma)/2$
Mixed aleatory–epistemic	$Pl_P = (1 - \gamma)/2$	$Pl_P = (1 - \gamma)/2$	$Pl_P = (1 - \gamma)/2$	$Bel_P = (1 + \gamma)/2$

are required for an accurate stochastic response surface according to Eq. (4). The inexpensive response surface replaces the deterministic model which proves to be computationally efficient in view of repetitive simulations required for DSTE analysis. This advantage is substantial for large scale computational models such as aerospace simulations including high fidelity models.

Based on the analysis presented by Shah et al. [35] for aleatory uncertainty discretization, the uniformly distributed variable  $x_1$  is

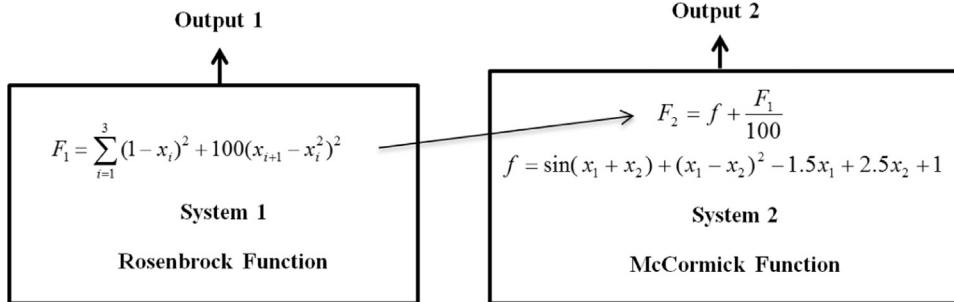


Fig. 5. Mathematical QMU problem.

Table 4

Uncertainty information for the mathematical QMU problem.

Variable	Distribution	Uncertainty information
$x_1$	Uniform	$[-0.5, 0.8]$
$x_2$	Epistemic	Source 1: $[-0.5, -0.1]$ 50%, $[0.1, 0.4]$ 50% Source 2: $[0.0, 0.5]$ 33.34%, $[-0.4, 0.2]$ 33.33%, $[-0.1, 0.1]$ 33.33% Source 3: $[0.25, 0.35]$ 35%, $[-0.45, -0.29]$ 65%
$x_3$	Normal	$N(0.25, 0.03)$
$x_4$	Epistemic	Source 1: $[0.2, 1.0]$ 30%, $[-1.0, 0.4]$ 70% Source 2: $[-0.2, 0.3]$ 33.34%, $[-0.5, -0.15]$ 33.33%, $[0.15, 0.9]$ 33.33%

segregated into 30 different intervals with an equal BPA of 1/30 for each sub-interval and the normally distributed variable is discretized into 20 intervals with BPA assigned to each sub-interval according to the Gaussian distribution shown in Eq. (16). The DSTE analysis is carried out with the composite Dempster–Shafer structure for mixed UQ for the design condition (see Fig. 6).

## 7.2. Performance gates and UQ for system 1

In this example problem, System 1 is considered to be bounded by both, upper and lower boundaries. The lower boundary consists of a normally distributed parameter, treated as a pure aleatory limit which provides a single CDF and the upper boundary for System 1 is represented by a 2 variable Booth function which is given by

$$FU_{sys1} = (y_1 + 2x_2 - 7)^2 + (2y_1 + x_2 - 5)^2 \quad (23)$$

where  $FU_{sys1}$  denotes the upper boundary for System 1. As can be seen from Eq. (23), the upper boundary has a shared input variable in the form of  $x_2$ . The input uncertainty information for the performance gates is given in Table 5.

As the variable  $x_2$  is an epistemic variable with a Dempster–Shafer structure and  $y_1$  represents aleatory uncertainty, uncertainty is quantified using DSTE with discretization process for the aleatory variable. In this case, normally distributed variable  $y_1$  is discretized into 75 intervals to carry out the DSTE analysis for the composite Dempster–Shafer structure using a 2nd order chaos expansion (see Fig. 7). Thus, only 12 original function evaluations were required with an over-sampling ratio of 2.

## 7.3. Performance gates and UQ for system 2

There exists an upper boundary for System 2 in the form of Dakota textbook problem [55] with 2 uncertain variables which is given by

$$FU_{sys2} = (x_1 - 1)^4 + (x_2 - 1)^4 \quad (24)$$

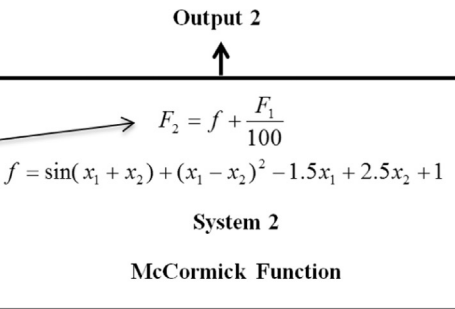


Fig. 5. Mathematical QMU problem.

Eq. (24) represents the same scenario as in the upper boundary for System 1. It shares an input variable  $x_1$  with the design condition, uncertainty data for which is shown in Table 4.  $x_2$  is an epistemic variable with a Dempster–Shafer structure from a single source as listed in Table 6.

As the upper boundary for System 2 is also characterized by mixed uncertainty, DSTE analysis is carried out by segregating the uniformly distributed variable  $x_1$  into 75 intervals with an equal BPA to each sub-interval (see Fig. 8). A 4th order chaos expansion with over-sampling ratio of 2 required 30 original function evaluations.

The surrogate models for each metric, including the performance gates, are compared to the original function output statistics in Figs. 6–8. It is evident that the NIPC response surfaces are accurate. Computational efficiency is also achieved in terms of original function evaluations which can be compared in Table 7.

## 7.4. Quantification of margins and uncertainties for QMU model problem

A confidence level of  $\gamma = 0.95$  is chosen for the QMU model problem. For better understanding, Fig. 9 gives a pictorial presentation for calculation of uncertainties and margins for System 1 with the specified confidence level. For System 1, QMU analysis based on upper and lower boundaries is summarized in Table 8.

Similarly for System 2, QMU analysis is solely based on the upper boundary which is summarized in Table 9. Thus, the system confidence ratio can be given as  $CR_{system} = \min\{CR_{sys1}, CR_{sys2}\} = 0.8319$ . We see that the confidence ratio for the whole system is governed by that of System 1, in particular the confidence ratio related to the lower

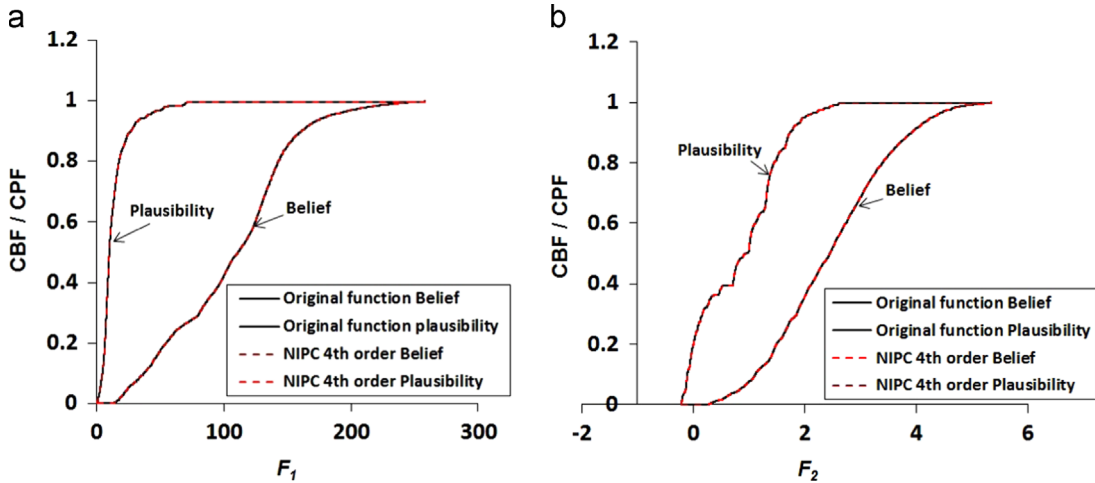


Fig. 6. Design condition for the QMU model problem. (a) System 1: design condition. (b) System 2: design condition.

Table 5

Input uncertainty information for the performance limits of System 1.

Lower boundary: Single parameter with  $N(-100.0, 5.5)$

Upper boundary

Variable	Distribution	Uncertainty information
$y_1$	Normal	$N(30.0, 2.5)$
$x_2$	Epistemic	Source 1: $[-0.5, -0.1]$ 50%, $[0.1, 0.4]$ 50% Source 2: $[0.0, 0.5]$ 33.34%, $[-0.4, 0.2]$ 33.33%, $[-0.1, 0.1]$ 33.33% Source 3: $[0.25, 0.35]$ 35%, $[-0.45, -0.29]$ 65%

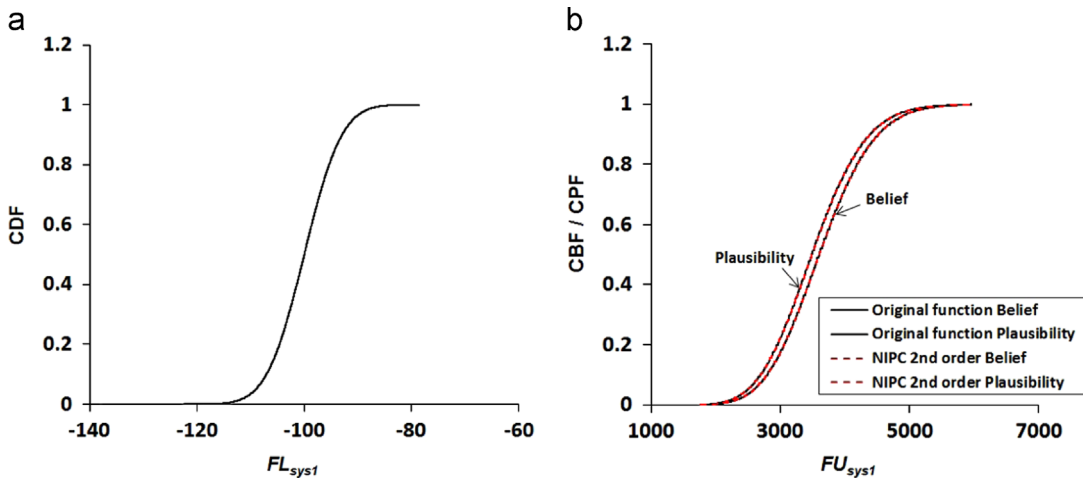


Fig. 7. Performance gates for System 1. (a) System 1: lower bound. (b) System 1: upper bound.

performance boundary and associated uncertainties including the design point. The parameter CR basically helps the decision-maker in risk assessment and risk mitigation. Post-analysis may be carried out on the basis of the confidence ratio parameter to make the design robust, which will be measured by the improvement in the confidence ratio.

## 8. Multidisciplinary analysis of a supersonic civil transport

A multidisciplinary analysis system for the high speed civil transport (HSCT) was selected as the 2nd model problem in order to

Table 6  
Uncertainty information for upper boundary of System 2.

Variable	Distribution	Uncertainty
$x_1$	Uniform	$[-0.5, 0.8]$
$z_2$	Epistemic	$[6.0, 6.5]$ 50%, $[6.3, 6.75]$ 30%, $[5.9, 6.2]$ 20%

demonstrate QMU using DSTE with stochastic expansions. The integrated multidisciplinary optimization object system (IMOO) [56], analysis tool used for this model problem, is a tool set designed to address many issues for next generation vehicle applications. It utilizes

an object-oriented integration framework that allows users to efficiently link high fidelity analysis modules. The problem setup time is significantly reduced by simplifying the definition of interdisciplinary coupling, allowing the creation of complex data objects and eliminating laborious manual data conversion. The IMOO system succeeds in sharing complex data by utilizing an object-oriented approach in which upstream modules create objects that are used by downstream modules on demand. Both the data and the methods reside in the object and downstream modules may request the data when needed. An example of this is mesh generation. IMOO implements automatic mesh generation and morphing through advanced parametric geometry and grid technology for multidisciplinary modeling [57]. M4 Engineering has developed a parametric grid morphing tool, geometry manipulation by automatic parameterization (GMAP [58]), and a

parametric finite element analysis (FEA) model generator for internal structures (RapidFEM [59]). These tools are integrated into the framework environment to quickly analyze FEA/CFD cases, morph geometry, re-mesh, apply loads, and generate useful results. Thus, the IMOO system allows configurations to be rapidly assessed and different numerical optimization techniques be used to help determine the optimal design.

### 8.1. Description of the deterministic model

For the current study, the analysis configuration selected is the HSCT [60] as shown in Fig. 10. The design variables used in the IMOO system model of the HSCT include the wing area, aspect ratio, sweep angle, taper ratio, span-wise location of break chord, leading edge position of break, break chord, and tip chord ratio (Fig. 11).

For the QMU demonstration, a modified version of the supersonic vehicle design process was chosen (shown in Fig. 12). The five modules considered are: (1) geometry, (2) aerodynamics, (3) propulsion, (4) structures and (5) range performance (Breguet range). The standard design structure matrix shows the analysis modules as blue boxes on the diagonal of the matrix, and the data items used by or generated by the modules are shown as yellow boxes. The far left column of yellow boxes represents inputs to the entire process, and the far right column represents outputs from the process. The outputs from a particular module are placed on the same row as the module, and the inputs are in the same column (e.g., propulsion performance is an output of the propulsion module and an input to the Breguet range module). In general, module execution is shuffled to get as much information as possible into the upper-right triangle of the matrix, which represents a feed-forward path, where the module generating the data is executed prior to the module using the data. Feedback paths are possible, but require special consideration (e.g., iteration to convergence) and hence, will not be included in this demonstration.

In this process, the geometry module takes the geometric variables and generates (through GMAP) an updated CFD model (via mesh morphing), a FEM mesh (through parametric geometry and meshing), and information for the propulsion module. Fig. 13(a) shows the initial geometry used to develop the baseline aerodynamic and structural meshes.

The aerodynamics module calculates the vehicle aerodynamic coefficients and distributed pressures at various flight conditions for use in performance simulation and load calculations. In order to expedite aerodynamic analyses, the current implementation of the aerodynamics module utilizes PANAIR [61] to compute aerodynamic loads. PANAIR (panel aerodynamics) solves the linearized potential flow

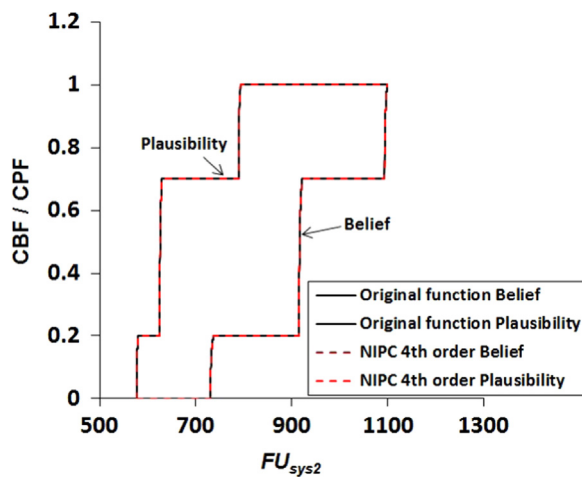


Fig. 8. Performance gate for System 2: upper bound.

**Table 7**  
Computational efficiency of NIPC methodology.

Performance metric	Polynomial order	Original function evaluations	Original function evaluations using NIPC
Design point: System 1	4	47 967	140
Upper bound: System 1	2	560	12
Design point: System 2	4	39 219	140
Upper bound: System 2	4	180	30

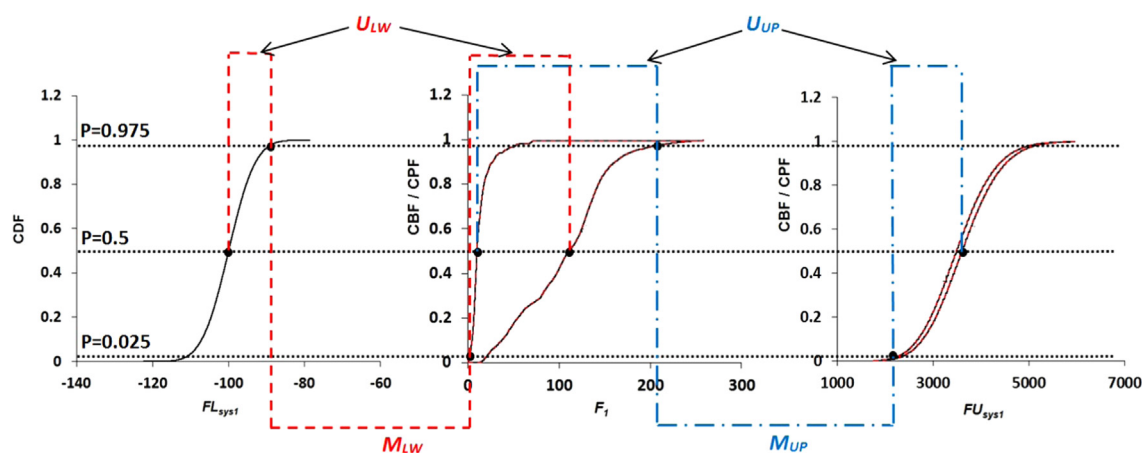


Fig. 9. Demonstration for calculation of uncertainties and margins for System 1. (Note that the figures are not drawn to scale to increase the clarity.)

problem for subsonic and supersonic regimes using a higher-order panel method [62–64]. Fig. 13(b) shows the half model used for aerodynamic analysis.

The propulsion module utilizes the numerical propulsion system simulation (NPSS) [65] to calculate the propulsion performance

**Table 8**  
System 1: QMU analysis metrics.

Performance gate	Margin	Uncertainty	CR
Lower	91.3959	109.859	0.8319
Upper	2124.765	1292.169	1.6443

**Table 9**  
System 2: QMU analysis metrics.

Performance gate	Margin	Uncertainty	CR
Upper	571.9426	339.7115	1.6836

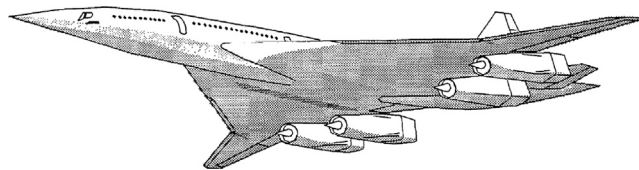


**Fig. 10.** Generic HSCT configuration.

- **High Speed Civil Transport (HSCT)**
- **Geometric Design Variables**
  - S (wing projected area)
  - AR (aspect ratio)
  - Sweep
  - Taper
  - Omega
  - Eta
  - Theta

Non-dimensional representation of wing break

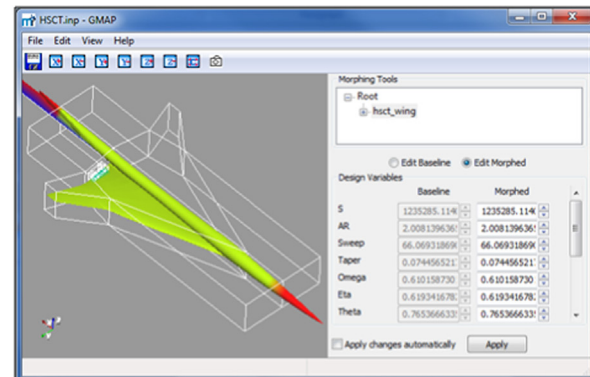


**Fig. 11.** HSCT with geometric design variables.

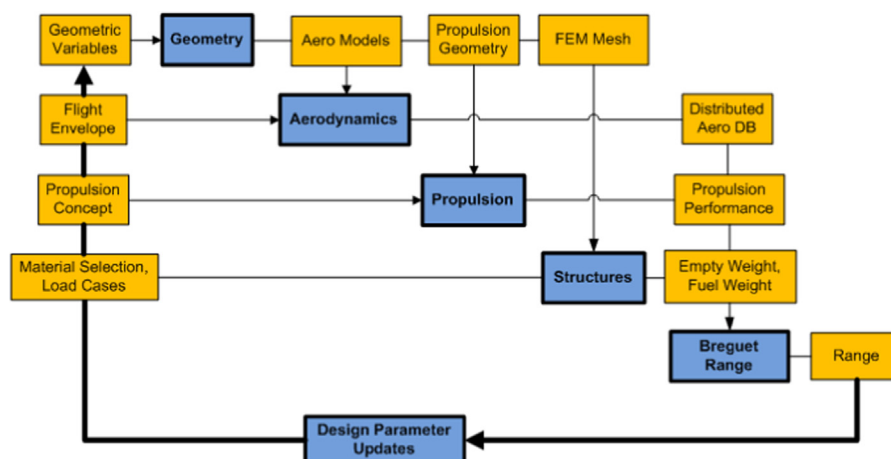


**Fig. 12.** Supersonic vehicle design structure matrix. (For interpretation of the references to color in this figure caption, the reader is referred to the web version of this paper.)

(specific fuel consumption etc.) for use in the Breguet range module. NPSS is a comprehensive propulsion simulation tool capable of accurately predicting aerothermodynamic behavior of jet engines in various flight regimes.

The structural module, using a NASTRAN optimization, calculates loads and structural sizing to estimate the takeoff gross weight (TOGW). The design load case simulated corresponds to a 1.5-g pull up (consistent with FAR part 25 criteria). The Breguet range module computes the range performance for the supersonic vehicle based upon the outputs from the upstream modules.

## 8.2. Description of the stochastic model

### 8.2.1. Design

For the HSCT model problem, two modules (geometry and aerodynamics) have been chosen to include uncertain input parameters. The schematic of the stochastic model for the HSCT problem is shown in Fig. 14. The geometry module has 2 uncertain input parameters: wing sweep angle and the wing taper ratio. The Mach number and the angle of attack, being the two important parameters in aerodynamic analysis, have been chosen as the source of uncertainty for the design of supersonic vehicle. The uncertainty information for all the parameters is summarized in Table 10.

Given the input uncertainty, the range and the drag coefficient are considered as the performance metrics which are related to multiple systems, each subject to inherent and epistemic uncertainties. The Range plays an important role in the design of a civil transport vehicle and coefficient of drag is one of the key design parameters that affects the vehicle performance.

### 8.2.2. Performance gates for the range

In an aircraft design, a minimum value of range for which the aircraft should fly is specified. For demonstration purposes, we select a lower boundary for the range as 2700 nautical miles (nmi) with no uncertainty.

### 8.2.3. Performance gates for the coefficient of drag

In aircraft design, a maximum value of drag coefficient may be used as a criteria to limit engine selection size and reduce fuel economy. In present analysis, drag coefficient is constrained by an upper limit of 0.0085 with no uncertainty.

## 8.3. Uncertainty quantification using DSTE

### 8.3.1. Design

UQ analysis for the HSCT design condition is carried out using the DSTE approach with stochastic expansions. As there are 4 uncertain variables in the system, according to Eq. (2), 30 deterministic evaluations were required with a  $n_p$  of 2 for a second order PCE. The taper

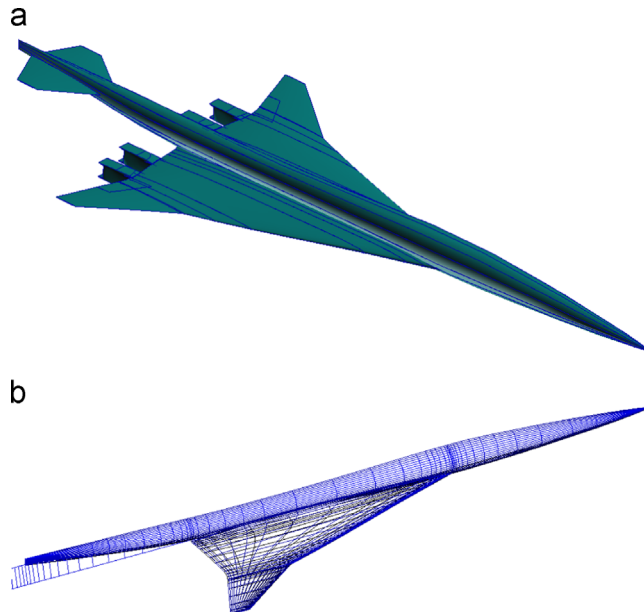


**Fig. 13.** HSCT: geometry and aerodynamics model. (a) HSCT base geometry (shown without vertical tail). (b) HSCT PANAIR model (wing body wake).

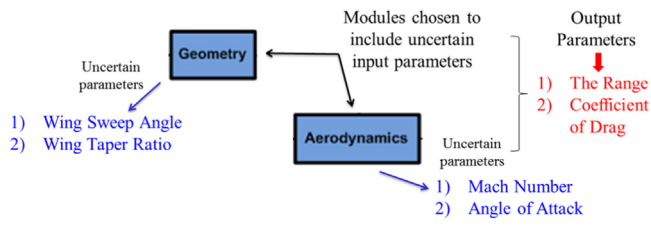


**Fig. 14.** Stochastic model for HSCT.

ratio was discretized into 23 sub-intervals and the Mach number and sweep angle were discretized into 22 sub-intervals each to obtain the belief and plausibility measures. The CBF and CPF for the output quantities, range and coefficient of drag are shown in Fig. 15.

To assess the accuracy of the response surface for range and coefficient of drag, 10 sample points were chosen in the uncertainty domain at which the difference between the actual model and the surrogate (i.e., the response surface) were calculated. It was found that the surrogate models for the range and coefficient of drag, based on a second order PCE, were accurate with the highest mean error being approximately 0.05%. As a result of this error analysis, the QMU analysis was performed using the second order expansion.

### 8.3.2. Performance limits

As mentioned before, no uncertainty was considered in case of performance gates for both the output quantities. Thus, they are treated as being constant which will correspond to the row with 'No uncertainty' in Tables 1–3.

## 8.4. Quantification of margins and uncertainties for HSCT

Now that the uncertainties are quantified in the design condition, the next step is to perform the QMU analysis on HSCT. Similar to the previous example problem, a confidence level of  $\gamma=0.95$  is chosen for the HSCT problem. The design metric for the range of the supersonic vehicle is represented by mixed uncertainty whereas the lower performance limit is attributed with no uncertainty. Using the equations and tables given in Section 6.2, the uncertainty and margin calculations are performed and summarized in Table 11 in terms of CR.

Similarly, the drag coefficient is also represented with mixed uncertainty whereas the upper performance limit has no uncertainty. The QMU analysis results are summarized in Table 12.

Using Eq. (22), system wide confidence ratio is the minimum CR from among the two output quantities under consideration. The minimum value is chosen as it indicates the weakest link in the system design. In present analysis, the system wide confidence ratio is obtained as 1.289 for coefficient of drag, indicating that the margins are greater than the uncertainties. In case the uncertainties are greater than or equal to the margins (i.e.,  $CR \leq 1$ ), a redesign of the system, performance limits or both may be required to make the system more reliable.

## 9. Conclusion

The objective of this paper is to implement Dempster–Shafer Theory of Evidence (DSTE) in the presence of mixed uncertainty to the system reliability and performance assessment of complex engineering systems through the use of quantification of margins and uncertainties (QMU) methodology. Specifically, uncertainty quantification (UQ) has been used as a tool of certification to decide whether a system is likely to perform safely and reliably within design specifications. Importance and contribution of the current study lies in creation of a novel QMU framework in terms of Dempster–Shafer structures (belief and plausibility) which can be used for performance

**Table 10**

HSCT uncertain parameters.

Variable	Distribution	Uncertainty information
Mach number ( $\tilde{M}$ )	Normal	$N(2.0, 0.02)$
Angle of Attack ( $\tilde{\alpha}$ )	Epistemic	Source 1: [2.4, 2.45] 20%, [2.43, 2.56] 50%, [2.51, 2.6] 30% Source 2: [2.58, 2.6] 10%, [2.5, 2.55] 60%, [2.45, 2.49] 30%
Wing sweep angle ( $\tilde{\lambda}$ )	Normal	$N(68.0, 1.0)$
Wing taper ratio ( $\lambda$ )	Uniform	[0.06, 0.1]

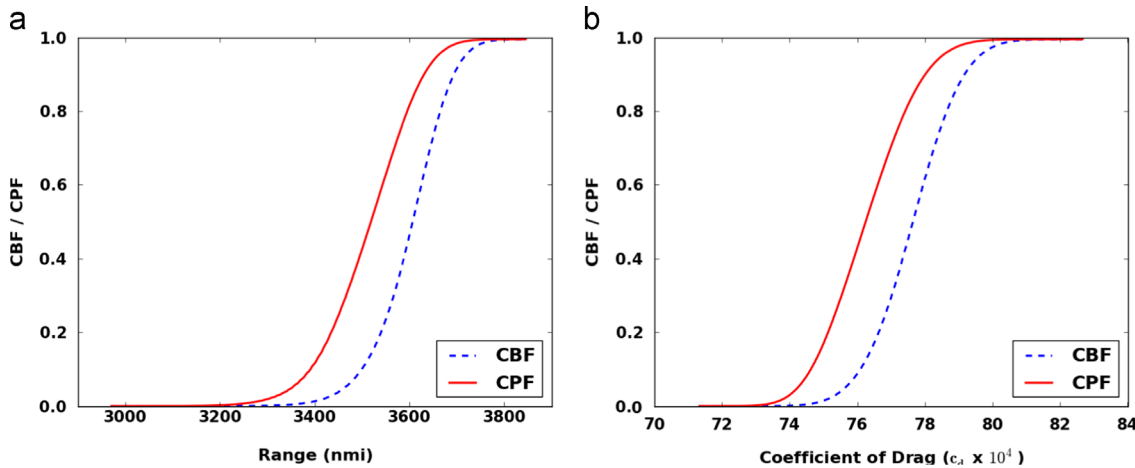


Fig. 15. UQ for HSCT using DSTE. (a) HSCT: range. (b) HSCT: coefficient of drag.

**Table 11**  
HSCT range: QMU analysis metrics.

Performance gate	Margin	Uncertainty	CR
Lower	611.951	289.347	2.1149

**Table 12**  
HSCT drag coefficient: QMU analysis metrics.

Performance gate	Margin	Uncertainty	CR
Upper	$5.085 \times 10^{-4}$	$3.947 \times 10^{-4}$	1.289

assessment of a system under uncertainty. Specifically, DSTE is used for uncertainty quantification to address the possibility of multiple sources and intervals for epistemic uncertainty characterization. Furthermore, the DSTE is utilized for mixed uncertainty quantification by discretizing the aleatory probability distributions into optimum sets of intervals and treating them as well-characterized epistemic variables. In addition, the response quantities of interest for design performance and boundaries are represented with stochastic surrogates based on non-intrusive polynomial chaos (NIPC) to reduce the computational expense of implementing DSTE for uncertainty quantification of high-fidelity complex system models.

The first QMU model problem consisted of a complex system of nonlinear functions which are typically used in numerical optimization studies. The QMU methodology using the evidence theory is demonstrated on the coupled analytical system of equations, which have shared inputs with their respective performance boundaries. In order to demonstrate the usage of evidence theory in propagating mixed uncertainties, different combinations of performance metrics and limits were adopted in the QMU analysis.

The second model problem was multi-disciplinary analysis of a high speed civil transport for the demonstration of the QMU methodology for complex engineering systems in aerospace applications. The drag coefficient and the range performance were studied as the output quantities which are considered critical during an aircraft design process. Second order NIPC expansions were used as surrogates for both performance metrics, which proved to be computationally efficient in quantifying the margins and uncertainties using evidence theory.

Overall, the proposed approach outlined a computationally efficient framework for quantifying margins and uncertainties with DSTE and stochastic expansions. Two model problems were utilized to demonstrate the QMU methodology, which included various types of uncertainty representations for the performance metrics and limits.

The results indicate the potential of the proposed QMU approach for the evaluation of safety and reliability of complex engineering systems in terms of efficiency and effectiveness.

## Acknowledgments

Funding for this research was provided by NASA Jet Propulsion Laboratory under a Small Business Technology Transfer Phase II Project Grant no. NNX11CC60C (Lee D. Peterson, program manager).

## References

- Sharp DH, Wood-Schultz MM. QMU and nuclear weapons certification. *What's under the hood*. Los Alamos Sci. 2003;28:47–53.
- Goodwin BT, Juzaitis RJ. National certification methodology for the nuclear weapon stockpile. Draft Working Paper; 2003.
- Eardley D. Quantification of margins and uncertainties (QMU). Technical Report, JSR-04-330 (JASON); March 2005.
- U.S. GAO (U.S. Government Accountability Office). Nuclear weapons: NNSA needs to refine and more effectively manage its new approach for assessing and certifying nuclear weapons. GAO-06-261. Washington, DC: U.S. Government Accountability Office; 2006.
- NAS/NRC (National Academy of Science/National Research Council). Evaluation of quantification of margins and uncertainties for assessing and certifying the reliability of the nuclear stockpile. Washington, DC: National Academy Press; 2008.
- Pilch M, Trucano TG, Helton JC. Ideas underlying the quantification of margins and uncertainties. *Reliab Eng Syst Saf* 2011;96:965–75.
- Pepin RJ, Rytherford AC, Hemez FM. Defining a practical QMU metric. In: 49th AIAA/ASME/ASCE/AHS/ASC structures, structural dynamics and materials conference, AIAA Paper 2008-1717, Schaumburg, IL; April 2008.
- Lucas LJ, Owhadi H, Ortiz M. Rigorous verification, validation, uncertainty quantification and certification through concentration-of-measure inequalities. *Comput Methods Appl Mech Eng* 2008;197(October (51–52)):4591–609.
- Iaccarino G, Pecnik R, Glimm J, Sharp D. A QMU approach for characterizing operability limits of air-breathing hypersonic vehicles. LANL Report, LA-UR 09-01863; 2009.
- National Research Council evaluation of quantification of margins and uncertainties methodology for assessing and certifying the reliability of the nuclear stockpile. Washington, DC: The National Academies Press; 2009.
- Helton JC. Quantification of margins and uncertainties: conceptual and computational basis. *Reliab Eng Syst Saf* 2011;96(9):976–1013.
- Oberkampf WL, DeLand SM, Rutherford BM, Diegert KV, Alvin KF. Error and uncertainty in modeling and simulation. *Reliab Eng Syst Saf* 2002;75:333–57.
- Urbina A, Mahadevan S, Paez TL. Quantification of margins and uncertainties of complex systems in the presence of aleatory and epistemic uncertainty. *Reliab Eng Syst Saf* 2011;96:1114–25.
- Wallstrom TC. Quantification of margins and uncertainties: a probabilistic framework. *Reliab Eng Syst Saf* 2011;96:1053–62.
- Helton JC, Johnson JD, Oberkampf WL, Storlie CB. A sampling-based computational strategy for the representation of epistemic uncertainty in model predictions with evidence theory. *Comput Methods Appl Mech Eng* 2007;196(37–40):3980–98.
- Owhadi H, Scovel C, Sullivan TJ, McKerns M, Ortiz M. Optimal uncertainty quantification. *SIAM Rev* 2013;55(2):271–345.

[17] Shafer G. *A mathematical theory of evidence*. Princeton, NJ: Princeton University Press; 1976.

[18] Pereira LC, Guimaraes LJN, Horowitz B, Sanchez M. Coupled hydro-mechanical fault reactivation analysis incorporating evidence theory for uncertainty quantification. *Comput Geotech* 2014;56:202–15.

[19] Helton JC, Johnson JD, Oberkampf WL, Sallaberry CJ. Representation of analysis results involving aleatory and epistemic uncertainty. *Int J Gen Syst* 2010;39(6):605–46.

[20] Helton JC, Oberkampf WL, Johnson JD. Competing failure risk analysis using evidence theory. *Risk Anal* 2005;25(4):973–95.

[21] Helton JC, Johnson JD. Quantification of margins and uncertainties: alternative representations of epistemic uncertainty. *Reliab Eng Syst Saf* 2011;96(9):1034–52.

[22] Swiler LP, Paez TL, Mayes RL, Eldred MS. Epistemic uncertainty in the calculation of margins. In: 50th AIAA/ASME/ASCE/AHS/ASC structures, structural dynamics and materials conference, AIAA Paper 2009-2249, Palm Springs, CA; May 2009.

[23] Bae H, Grandhi RV, Canfield RA. An approximation approach for uncertainty quantification using evidence theory. *Reliab Eng Syst Saf* 2004;86:215–25.

[24] Bae H, Grandhi RV, Canfield RA. Epistemic uncertainty quantification techniques including evidence theory for large-scale structures. *Reliab Eng Syst Saf* 2004;82:1101–12.

[25] Agarwal H, Renaud JE, Padmanabhan D. Uncertainty quantification using evidence theory in multidisciplinary design optimization. *Reliab Eng Syst Saf* 2004;85:281–94.

[26] Hosder S, Walters RW, Balch M. Efficient sampling for non-intrusive polynomial chaos applications with multiple input uncertain variables. In: 9th AIAA non-deterministic approaches conference, AIAA Paper 2007-1939, Honolulu, HI; April 2007.

[27] Hosder S, Walters RW, Balch M. Point-collocation non-intrusive polynomial chaos method for stochastic computational fluid dynamics. *AIAA J* 2010;48(December (12)):2721–30.

[28] Bettis BR, Hosder S, Winter T. Efficient uncertainty quantification in multidisciplinary analysis of a reusable launch vehicle. In: 17th AIAA international space planes and hypersonic systems and technologies conference, AIAA Paper 2011-2393, San Francisco, CA; April 2011.

[29] Hosder S. Stochastic response surfaces based on non-intrusive polynomial chaos for uncertainty quantification. *Int J Math Model Numer Optim* 2012;3(January (1–2)):117–39.

[30] Hosder S, Bettis BR. Uncertainty and sensitivity analysis for reentry flows with inherent and model-form uncertainties. *J Spacecr Rocket*. 2012;49(March–April (2)):193–206.

[31] Eldred MS, Swiler LP, Tang G. Mixed aleatory-epistemic uncertainty quantification with stochastic expansions and optimization-based interval estimation. *Reliab Eng Syst Saf* 2011;96:1092–113.

[32] Helton JC, Johnson JD, Sallaberry CJ. Quantification of margins and uncertainties: example analyses from reactor safety and radioactive waste disposal involving the separation of aleatory and epistemic uncertainty. *Reliab Eng Syst Saf* 2011;96(9):1014–33.

[33] Sentz K, Ferson S. Probabilistic bounding analysis in the quantification of margins and uncertainties. *Reliab Eng Syst Saf* 2011;96:1126–36.

[34] Ferson S, Kreinovich V, Ginzburg L, Meyers DS, Sentz K. Constructing probability boxes and Dempster–Shafer structures. Sandia National Laboratories SAND2002-4015, Albuquerque, NM; 2002.

[35] Shah HR, Hosder S, Winter T. A mixed uncertainty quantification approach with evidence theory and stochastic expansions. In: AIAA SciTech 2014, AIAA Paper 2014-0298, National Harbor, MD; January 2014.

[36] Parry GW, Winter PW. Characterization and evaluation of uncertainty in probabilistic risk analysis. *Nucl Saf* 1981;22(1):28–42.

[37] Parry GW. The characterization of uncertainty in probabilistic risk assessments of complex systems. *Reliab Eng Syst Saf* 1996;54(2–3):119–26.

[38] Pate-Cornell ME. Uncertainties in risk analysis: six levels of treatment. *Reliab Eng Syst Saf* 1996;54(2–3):95–111.

[39] Hoffman FO, Hammonds JS. Propagation of uncertainty in risk assessments: the need to distinguish between uncertainty due to lack of knowledge and uncertainty due to variability. *Risk Anal*. 1994;14(5):707–12.

[40] Helton JC, Burmaster DE. Guest editorial: treatment of aleatory and epistemic uncertainty in performance assessments for complex systems. *Reliab Eng Syst Saf* 1996;54(2–3):91–4.

[41] Helton JC. Uncertainty and sensitivity analysis in the presence of stochastic and subjective uncertainty. *J Stat Comput Simul* 1997;57(1–4):3–76.

[42] Helton JC. Treatment of uncertainty in performance assessments for complex systems. *Risk Anal* 1994;14(4):483–511.

[43] Oberkampf WL, Helton JC, Sentz K. Mathematical representation of uncertainty. In: 3rd AIAA non-deterministic approaches forum, AIAA Paper 2001-1645, Seattle, WA; April 2001.

[44] Xiu D, Karniadakis GE. The Wiener–Askey polynomial chaos for stochastic differential equations. *SIAM J Sci Comput* 2003;24(2):619–44.

[45] Xiu D, Karniadakis GE. Modeling uncertainty in flow simulations via generalized polynomial chaos. *J Comput Phys* 2003;187(1):137–67.

[46] Najm HN. Uncertainty quantification and polynomial chaos techniques in computational fluid dynamics. *Ann Rev Fluid Mech* 2009;41:35–52.

[47] Ghanem RG, Spanos P. *Stochastic finite elements: a spectral approach*. Berlin: Springer; 1991.

[48] Eldred MS, Webster CG, Constantine PG. Evaluation of non-intrusive approaches for Wiener–Askey generalized polynomial chaos. In: 10th AIAA non-deterministic approaches forum, AIAA-Paper 2008-1892, Schaumburg, IL; April 2008.

[49] Yager R. Arithmetic and other operations on Dempster–Shafer structures. *Int J Man-Mach Stud* 1986;25:357–66.

[50] Zadeh LA. Review of books: a mathematical theory of evidence. *AI Mag* 1984;5(3):81–3.

[51] Sentz K, Ferson S. Combination of evidence in Dempster–Shafer theory. Sandia National Laboratories SAND2002-0835, Albuquerque, NM; April 2002.

[52] Zadeh LA. A simple view of the Dempster–Shafer theory of evidence and its implication for the rule of combination. *AI Mag* 1986;7:85–90.

[53] Helton JC, Johnson JD, Oberkampf WL. An exploration of alternative approaches to the representation of uncertainty in model predictions. *Reliab Eng Syst Saf* 2004;85:39–71.

[54] Nikolaidis E, Ghiocel DM, Singhal S. *Engineering design reliability handbook*. 1st ed. Boca Raton, FL: CRC Press; 2004 [July, Chapter 10].

[55] Adams BM, Ebeida MS, Eldred MS, Jakeman JD, Swiler LP, Bohnhoff WJ, et al. Dakota, a multilevel parallel object-oriented framework for design optimization, parameter estimation, uncertainty quantification, and sensitivity analysis. Sandia National Laboratories SAND2010-2183, Albuquerque, NM, Updated March 6, 2014.

[56] Doyle S, PMP KA, Winter T. Developing the aerodynamics module for the integrated multidisciplinary optimization object system. In: 49th AIAA aerospace sciences meeting including the new horizons forum and aerospace exposition. AIAA Paper 2011-8, Orlando, FL; January 2011.

[57] Raymondson C, Baker M, Doyle S, Young S, Teijel D. Geometry manipulation by automatic parameterization (GMAP). AIAA MDAO conference; September 2008.

[58] Dahlin Andrew, Baker Myles L. *GMAP mesh user's manual s.1*. Long Beach, CA: M4 Engineering; 2010.

[59] Stuewe Daniel, Baker Myles L. *Rapid FEM user's manual*. Long Beach, CA: M4 Engineering; 2010.

[60] High Speed Research Program HSR II Airframe Task 20, Task 2.1 Technology Integration, Sub-task 2.1.1.2 Refine Technology Concept Airplane: Configuration Description Document; April 1996.

[61] Saaris GR, Tinoco EN, Lee JL, Rubbert PE. User's guide PAN AIR technology program for solving potential flow about arbitrary configurations; 1992.

[62] Johnson FT, Rubbert PE. Advanced panel-type influence coefficient methods applied to subsonic flows. s.l. AIAA 75-50; January 1975.

[63] Ehlers FE, Johnson FT, Rubbert PE. A higher order panel method for linearized supersonic flow. s.l. AIAA 76-381; July 1976.

[64] Ehlers FE, et al. A higher order panel method for linearized supersonic flow. NASA Contractor Report 3062; 1979.

[65] Claus RW, Evans AL, Lylte JK, Nichols LD. Numerical propulsion system simulation. 4. *Comput Syst Eng* 1991;2:357–64.